Design Of 2x2 MIMO Antenna with Improved Isolation For 4.2 GHz Frequency Applications

P. Vinay Kumar[1], P. Manikanta Krishna Babu[2], M. Venkata Srinivas[3], B. Deepak Kumar[4]
[1,2,3,4] *Department of Electronics and Communication Engineering, Vasireddy Venkatadri Institute of Technology, Guntur, India*

***Abstract*—This paper describes a 2×2 MIMO microstrip patch antenna for 4.2 GHz C-band applications, fabricated on Rogers RT5880 (ε_r = 2.2, h = 1.6 mm) within a 60 × 60 mm² footprint. Mutual coupling is managed through corner-truncated patches and a vertical stub; the stub introduces reverse-phase currents to reduce electromagnetic interaction between ports. CST simulations show a return loss (S_{11}) of −35.2 dB and isolation (S_{21}) exceeding −18 dB. The Envelope Correlation Coefficient of 0.002 confirms that the two ports are effectively decorrelated, making the design viable for spatial diversity in wireless communication and radar applications.**

***Index Terms*—Envelope Correlation Coefficient (ECC), Isolation, Microstrip patch, MIMO antenna, Mutual coupling, Stub technique.**

I. INTRODUCTION

Wireless systems demand higher data rates and improved reliability across difficult channels [3], [24]. MIMO has become the standard response, particularly in C-band [24]. Multiple antenna elements improve spectral efficiency and handle multipath fading without additional power or bandwidth [1], [11],[19],[30].

Compact MIMO designs, however, run into a consistent problem: mutual coupling. When elements are placed close together, electromagnetic interaction between them degrades return loss, radiation efficiency, and ECC [2], [4]. Controlling this coupling is what separates a functional MIMO system from one that only approaches its theoretical limits on paper [7], [25].

Existing solutions parasitic elements [14], defected ground structures, EBG structures [26] are effective but typically add fabrication complexity or alter the radiation pattern. This paper proposes a 2×2 MIMO microstrip patch antenna at 4.2 GHz that uses corner truncation combined with stub-based decoupling. The stub introduces reverse-phase currents to cancel inter-port coupling [6]. Design and simulation were carried out in CST Studio Suite [10]; subsequent sections cover the methodology and diversity performance analysis.

II. LITERATURE REVIEW

A. Review of Microstrip Patch Antennas

Microstrip patch antennas remain a practical choice in wireless design, compact, planar, and straightforward to fabricate on printed circuit boards. Pozar [21], Balanis [22], Chen [15], and Stutzman and Thiele [16] collectively cover the theoretical and design foundations of microstrip antenna systems. Wong [12] showed that low-dielectric substrates increase radiation efficiency and bandwidth. Slot loading, parasitic elements, and alternative feeding techniques have also been used for better impedance matching and multiband operation [12], [23]. Beyond standard rectangular patches, microstrip geometries have been extended to octagonal [13], wearable [17], slot-based [28], and fractal configurations [29], each addressing specific performance trade-offs. Beamforming and array applications have also drawn on microstrip designs [18], [19], and metamaterial-based enhancements have been explored to push performance further [5]. Bandwidth and gain, however, remain the persistent constraints across most configurations at high frequencies.

B. Mutual Coupling and Its Effects

In MIMO systems, multiple elements are packed close together to boost channel capacity [24], which introduces mutual coupling. The elements interact electromagnetically, causing power leakage and inter-port interference. Chae et al. [4] showed that this degrades return loss, radiation efficiency, and correlation characteristics all of which directly affect diversity performance.

C. Techniques for Mutual Coupling Reduction

DGS structures disrupt surface currents to improve isolation, while EBG structures block inter-element interference at the source [26]. Parasitic elements achieve similar results with less structural overhead [14], and strong isolation in compact MIMO configurations has been demonstrated for 5G applications as well [20]. Stub loading works differently the stub generates counter-phase currents that partially cancel the coupling field, improving isolation without adding to the antenna footprint [6], [8].

III. ANALYSIS OF ANTENNA DESIGN

The antenna is a two-port MIMO microstrip patch design for 4.2 GHz, fabricated on Rogers RT5880 ($\varepsilon_r = 2.2$, h = 1.6 mm) a substrate picked for its low loss tangent and predictable behavior at microwave frequencies. Two rectangular patches share a common substrate, fed by microstrip lines over a bottom ground plane. The design started as a single patch tuned to 4.2 GHz, then a second identical element was added to form the MIMO pair. Packing them close together introduces mutual coupling, which is brought down using corner truncation and stub loading. CST Studio Suite was used for simulation, with the design assessed on S_{11}, S_{21}, gain, radiation pattern, efficiency, and ECC.

$$W = \frac{c}{2f_0}\sqrt{\frac{2}{\varepsilon_r+1}} \quad (1)$$

$$\varepsilon_{eff} = \frac{\varepsilon_r+1}{2} + \frac{\varepsilon_r-1}{2}\left(1+12\frac{h}{W}\right)^{-1/2} \quad (2)$$

$$L_{eff} = \frac{c}{2f_0\sqrt{\varepsilon_{eff}}} \quad (3)$$

$$\Delta L = 0.412h\frac{(\varepsilon_{eff}+0.3)(\frac{W}{h}+0.264)}{(\varepsilon_{eff}-0.258)(\frac{W}{h}+0.8)} \quad (4)$$

$$L = L_{eff} - 2\Delta L \quad (5)$$

TABLE I Optimized Dimension of Single Element

Parameter	Dimensions (mm)	Parameter	Dimensions (mm)
W_P	28.5	L_P	23.5
W_F	4.8	L_F	12
C_w	2.5	h	1.6
S_L	60	S_W	60
Ins_L	8.5	Ins_W	6

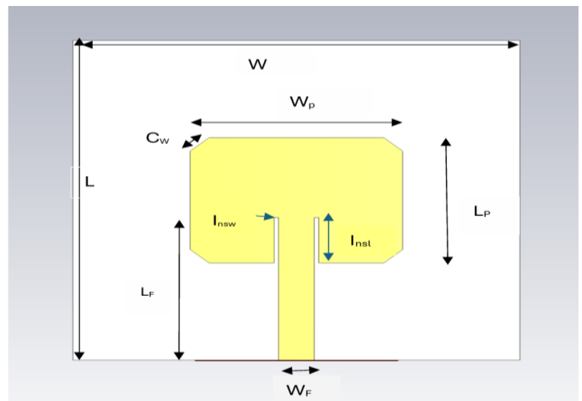

Figure 1. Single Element Geometry

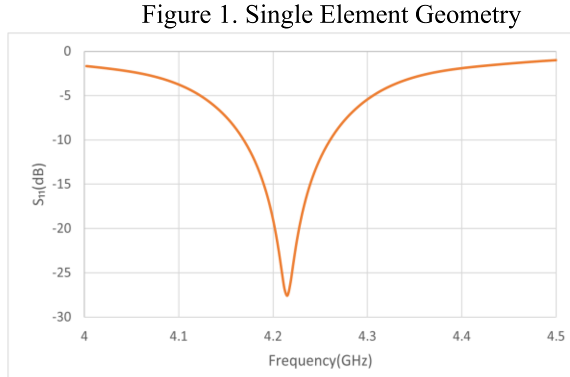

Figure 2. S_{11} of Single Patch

Adding a second patch close to the first creates immediate problems. The two elements interact electromagnetically, and that interaction shows up across every key parameter isolation drops, S_{11} shifts, current distribution changes. The resonant frequency drifts slightly from the target, and impedance matching degrades. This is the baseline problem the decoupling stage is designed to fix.

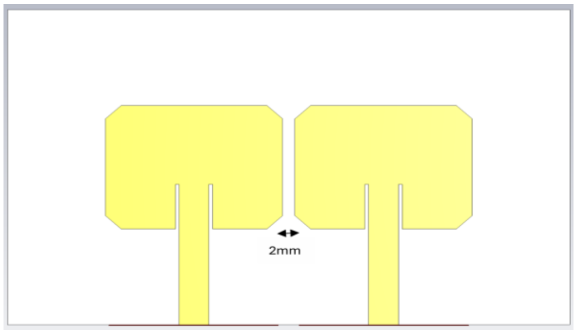

Figure 3. MIMO Antenna without stub

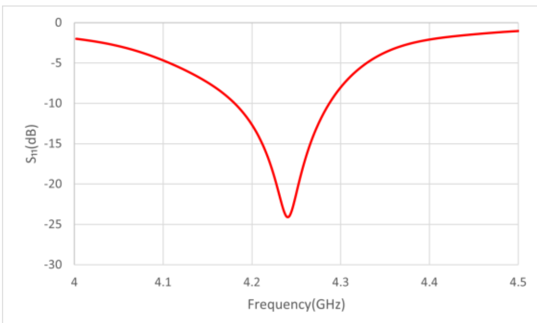

Figure 4. S_{11} before placing stub

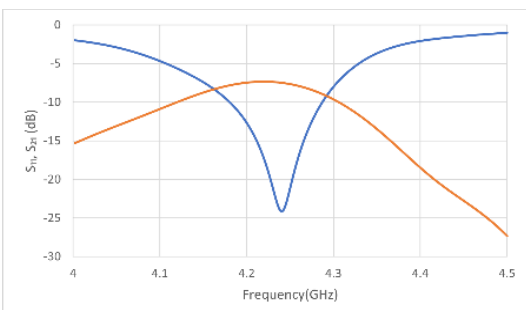

Figure 5. S_{11} & S_{21} before placing stub

The two patches are separated by 2 mm tight enough for a compact footprint, but at that distance the near-field interaction is strong. Surface currents from one element bleed into the other, driving mutual coupling up. S_{11} degrades as the adjacent element disturbs the impedance match, and the resonant frequency shifts slightly off target. Radiation pattern distortion and reduced efficiency follow from the non-uniform current distribution that results.

The incorporation of the stub structure provides a simple and effective solution for enhancing isolation in compact MIMO antenna systems without increasing design complexity. A significant improvement in performance is observed even at the small spacing of 2 mm. The stub acts as a reactive decoupling element that generates opposite phase currents, effectively canceling the coupled fields between the patches.

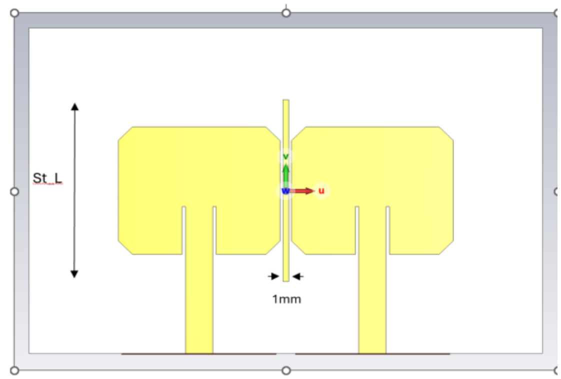

Figure 6. MIMO Antenna without stub

As a result, the isolation improves and demonstrating a substantial reduction in mutual coupling. The return loss also improves that to indicating enhanced impedance matching. Furthermore, the radiation pattern remains stable, and antenna efficiency is preserved.

Table Ii
Dimensions Of Antenna with Stub and Without Stub

Parameter	Dimensions(mm)	
	With Stub	Without stub
Antenna Size(mm)^2	60x60	60x60
Stub Length (St_L)	33.5	--
Stub width (St_w)	1	--

The stub structure has a clear impact on isolation performance. This is evident when comparing the S_{21} parameter of the MIMO antenna before and after adding the stub. The stub serves as a reactive decoupling element that changes the current distribution and creates opposite phase currents. This effectively cancels out the coupled signals. As a result, adding the stub greatly improves isolation without increasing the antenna size or making the design more complicated.
The stub's presence yields superior port decoupling, confirmed by the attenuated S_{21} response in modified designs. It strategically alters current flows to generate phase-opposed fields, neutralizing unwanted signal bleed.

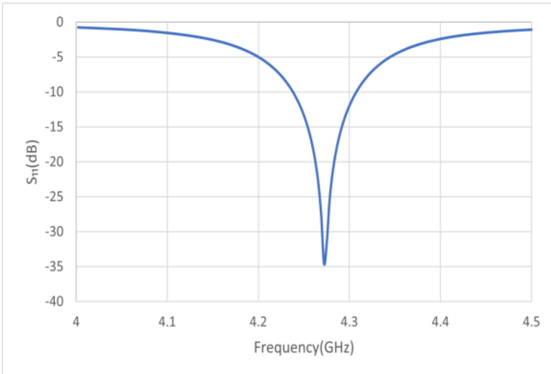

Figure 7. S_{11} after placing stub

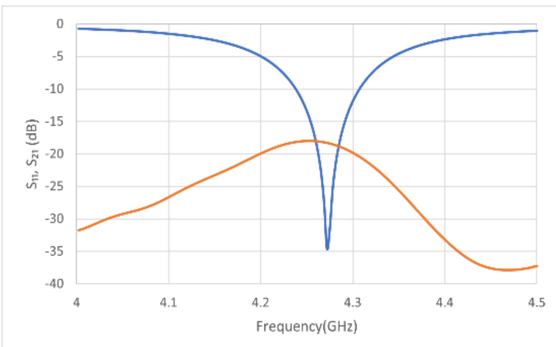

Figure 8. S_{11} & S_{21} after placing stub

Overall, the incorporation of the stub leads to better signal integrity, improved antenna efficiency, and lower correlation, making the MIMO system more suitable for high-performance wireless applications

IV. RESULTS AND DISCUSSION

Return loss, mutual coupling, and radiation pattern are compared across two configurations without stub and with stub to assess the effect of the isolation technique. Without any isolation mechanism, the radiation pattern distorts noticeably. At 2 mm separation, the near-field interaction between elements is strong enough to produce uneven surface current distribution, which degrades radiation performance. Efficiency takes a hit too coupling losses cause unwanted power transfer between the patches, reducing how much is actually radiated.

The S_{11} response before stub introduction shows resonance near 4.2 GHz, but the adjacent element pulls the impedance match off. The return loss is shallower than the single patch baseline, and the S_{21} stays high meaning significant power is leaking between ports rather than being radiated. This is the pre-stub baseline: the antenna resonates, but the two ports are not behaving independently.

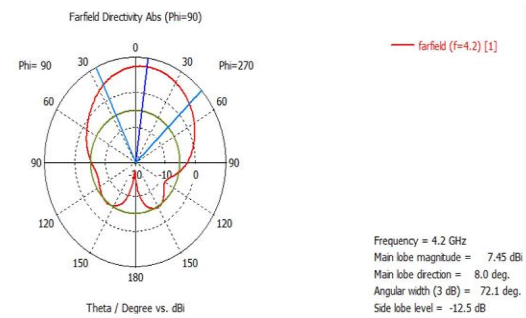

Figure 9. Radiation pattern without stub

Adding the stub changes this. The radiation pattern tightens up and closely resembles the single patch response (Fig. 10). The main lobe points broadside, the pattern stays roughly omnidirectional in the azimuth plane, side lobes reduce, and symmetry is maintained behavior typical of microstrip patch antennas [21], [22]. The improvement traces directly to reduced mutual coupling, which restores uniform current distribution [4].

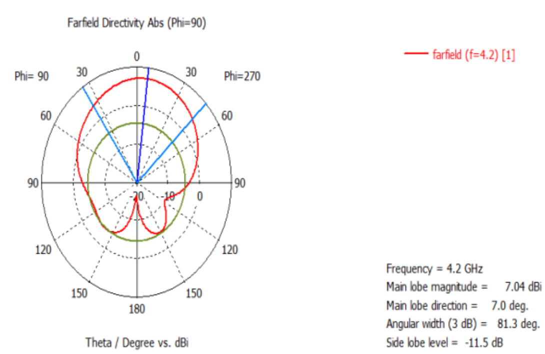

Figure 10. Radiation pattern with stub

Efficiency at 4.2 GHz reaches approximately 80% (Fig. 11). Total efficiency is somewhat lower due to residual impedance mismatch, but it holds steady across the band without any sharp drops. The degradation at higher frequencies is gradual and stays within acceptable limits.

Worth noting is that the efficiency gap between the stub and no-stub configurations is not marginal without the stub, coupling losses actively pull power away from radiation. The stub doesn't just improve isolation; it recovers efficiency that would otherwise be lost to inter-element interference. At 4.2 GHz specifically, this difference is most pronounced, which makes sense given that the stub is tuned to operate at that frequency.

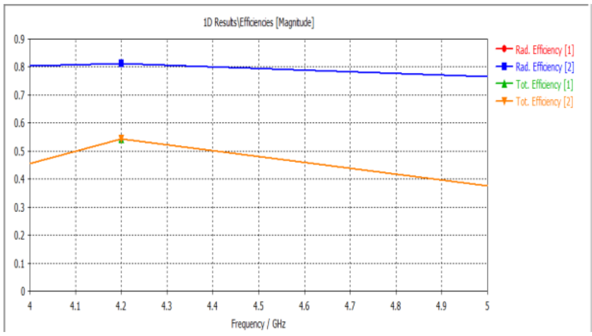

Figure 11. Efficiency pattern

The ECC stays below 0.1 across the entire operating band and approaches zero at 4.2 GHz (Fig. 12). This means the two ports are effectively decorrelated they operate independently with minimal electromagnetic interaction. The stub is primarily responsible for this; by reducing inter-element coupling, it brings the ECC down to near-zero at resonance, confirming solid diversity performance.

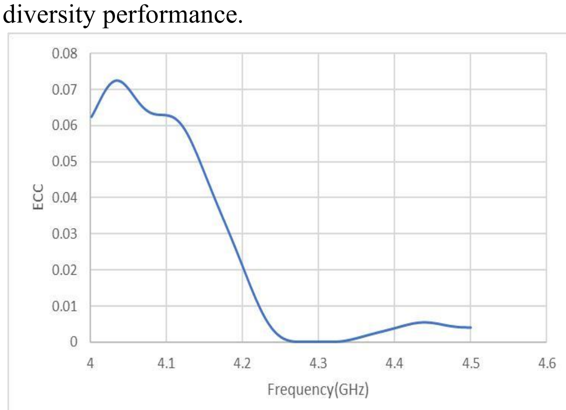

Figure 12. ECC Result of MIMO Antenna

V. CONCLUSION

A 2×2 MIMO microstrip patch antenna for 4.2 GHz was designed, simulated, and evaluated on Rogers RT5880 ($\varepsilon_r = 2.2$, h = 1.6 mm) within a 60 × 60 mm² footprint. The central challenge mutual coupling at 2 mm inter-element spacing was addressed using a combination of corner truncation and stub-based decoupling.

The stub proved effective. S_{11} reached −35.2 dB at the target frequency, S_{21} dropped below −18 dB across the operating band, and the ECC settled near zero at 4.2 GHz well below the 0.1 threshold required for MIMO diversity operation. Radiation efficiency held at approximately 80%, and the pattern remained stable and symmetric after stub introduction, closely matching the single-element baseline.

The results show that stub loading achieves meaningful isolation improvement without increasing antenna size or adding fabrication complexity a practical advantage for compact MIMO integration. The design is suitable for C-band wireless communication and radar applications where spatial diversity and low inter-port correlation are required.

REFERENCES

[1] M. S. Sharawi, Printed MIMO Antenna Systems: Performance Metrics, Theory and Design. Norwood, MA, USA: Artech House, 2014.

[2] S. Blanch, J. Romeu, and I. Corbella, "Exact representation of antenna system diversity performance from input parameters," Electronics Letters, vol. 39, no. 9, pp. 705–707, May 2003.

[3] J. G. Andrews, S. Buzzi, W. Choi, S. V. Hanly, A. Lozano, A. C. K. Soong, and J. C. Zhang, "What will 5G be?" IEEE Journal on Selected Areas in Communications, vol. 32, no. 6, pp. 1065–1082, Jun. 2014.

[4] S. H. Chae, S. K. Oh, and S. O. Park, "Analysis of mutual coupling, correlations, and efficiencies of MIMO antennas," IEEE Transactions on Antennas and Propagation, vol. 55, no. 11, pp. 3016–3025, Nov. 2007.

[5] R. Marqués, F. Medina, and R. Rafii-El-Idrissi, "Role of bianisotropy in negative permeability and left-handed metamaterials," Physical Review B, vol. 65, no. 14, pp. 144440, Apr. 2002.

[6] K. Wei, J. Li, L. Wang, Z. Xing, and R. Xu, "A meta-surface wall for mutual coupling reduction between two microstrip antennas," IEEE Antennas and Wireless Propagation Letters, vol. 13, pp. 1152–1155, 2014.

[7] M. S. Sharawi, "Printed multi-band MIMO antenna systems and their performance metrics," IEEE Antennas and Propagation Magazine, vol. 55, no. 5, pp. 218–232, Oct. 2013.

[8] A. Pandey, R. Verma, and A. K. Singh, "A four elements planar compact UWB MIMO antenna

with WLAN band rejection capabilities," International Journal of Electronics and Communications, vol. 114, pp. 152997, Mar. 2020.

[9] K. L. Wong, Planar Antennas for Wireless Communications. New York, NY, USA: John Wiley & Sons, 2003.

[10] Dassault Systèmes, CST Studio Suite User Manual. Vélizy-Villacoublay, France: Dassault Systèmes, 2023.

[11] M. S. Sharawi, Printed Multi-Antenna Systems for Wireless Terminals. Norwood, MA, USA: Artech House, 2014.

[12] K. L. Wong, Compact and Broadband Microstrip Antennas. New York, NY, USA: John Wiley & Sons, 2002.

[13] R. Q. Lee and K. F. Lee, "Experimental study of the octagonal microstrip antenna," in Proc. IEEE Antennas and Propagation Society Int. Symp., Syracuse, NY, USA, Jun. 1988, vol. 1, pp. 344–347.

[14] K. S. Vishvaksenan, K. Mithra, R. Kalaiarasan, and R. V. Rajeswari, "Mutual coupling reduction in microstrip MIMO antenna arrays using parasitic elements," IEEE Antennas and Wireless Propagation Letters, vol. 16, pp. 1557–1560, 2017.

[15] Z. N. Chen, Ed., Handbook of Antenna Technologies. Singapore: Springer, 2016.

[16] W. L. Stutzman and G. A. Thiele, Antenna Theory and Design, 3rd ed. Hoboken, NJ, USA: John Wiley & Sons, 2012.

[17] M. Tanaka and J. H. Jang, "Wearable microstrip antenna," in Proc. IEEE Antennas and Propagation Society Int. Symp., Columbus, OH, USA, Jun. 2003, vol. 2, pp. 22–27.

[18] L. C. Godara, "Application of antenna arrays to mobile communications, Part II: Beam-forming and direction-of-arrival considerations," Proc. IEEE, vol. 85, no. 8, pp. 1195–1245, Aug. 1997.

[19] P. S. Hall and S. J. Vetterlein, "Review of radio frequency beamforming techniques for MIMO," IET Microwaves, Antennas & Propagation, vol. 137, no. 5, pp. 293–303, Oct. 1990.

[20] R. Hussain and M. S. Sharawi, "A cognitive radio MIMO antenna system with strong isolation for 5G applications," IEEE Antennas and Wireless Propagation Letters, vol. 16, pp. 2494–2497, 2017.

[21] D. M. Pozar, "Microstrip antennas," Proc. IEEE, vol. 80, no. 1, pp. 79–91, Jan. 1992.

[22] C. A. Balanis, Antenna Theory: Analysis and Design, 3rd ed. Hoboken, NJ, USA: John Wiley & Sons, 2005.

[23] [23] R. Garg, P. Bhartia, I. Bahl, and A. Ittipiboon, Microstrip Antenna Design Handbook. Norwood, MA, USA: Artech House, 2001.

[24] G. J. Foschini and M. J. Gans, "On limits of wireless communications in a fading environment when using multiple antennas," Wireless Personal Communications, vol. 6, no. 3, pp. 311–335, Mar. 1998.

[25] E. Telatar, "Capacity of multi-antenna Gaussian channels," European Transactions on Telecommunications, vol. 10, no. 6, pp. 585–595, Nov. 1999.

[26] F. Yang and Y. Rahmat-Samii, "Microstrip antennas integrated with electromagnetic band-gap (EBG) structures: A low mutual coupling design for array applications," IEEE Transactions on Antennas and Propagation, vol. 51, no. 10, pp. 2936–2946, Oct. 2003.

[27] A. Diallo, C. Luxey, P. Le Thuc, R. Staraj, and G. Kossiavas, "Study and reduction of the mutual coupling between two mobile phone PIFAs operating in the DCS1800 and UMTS bands," IEEE Transactions on Antennas and Propagation, vol. 54, no. 11, pp. 3063–3074, Nov. 2006.

[28] S. I. Latif, L. Shafai, and S. K. Sharma, "Bandwidth enhancement and size reduction of microstrip slot antennas," IEEE Transactions on Antennas and Propagation, vol. 53, no. 3, pp. 994–1003, Mar. 2005.

[29] J. Anguera, C. Puente, C. Borja, and J. Soler, "Fractal-shaped antennas: A review," Wiley Encyclopedia of RF and Microwave Engineering, vol. 2, pp. 1620–1635, 2005.

[30] M. A. Jensen and J. W. Wallace, "A review of antennas and propagation for MIMO wireless communications," IEEE Transactions on Antennas and Propagation, vol. 52, no. 11, pp. 2810–2824, Nov. 2004.